Electronic Supplementary Information for

Boosting the Hydrodeoxygenation of PET Waste to Cycloalkanes by Electron Transfer and Hydrogen Spillover in H_xWO_{3-y} Incorporated Dendritic Fibrous Nanosilica Supported Ni Catalysts

Wenfeng Zhong,[a, b, d] Jiayi Wang,[b, d] Xuecheng Li,[b, d] Suhua Wang,[c,d] Hua Tan,[*, b, d] Xinping Ouyang,[*, a]

a. School of Chemistry & Chemical Engineering, South China University of Technology, Guangzhou 510640, P. R. China.

b. College of Chemistry, Guangdong University of Petrochemical Technology, Maoming 525000, P. R. China

c. School of Environmental Science and Engineering, Guangdong University of Petrochemical Technology, Maoming 525000, P. R. China

d. Guangdong Provincial Key Laboratory for Green Agricultural Production and Intelligent Equipment, Maoming 525000, P. R. China

Corresponding Authors: Xinping Ouyang: ceouyang@scut.edu.cn;

Hua Tan: huatan@gdupt.edu.cn

Table S1 Calibration data of all products obtained from the HDO of PET.

Chemicals	Calibration data	R^2	GC response factor
Cyclohexane	$y=2.10399\times10^7x-36941.46$	0.98	2.10399×10^7
Methylcyclohexane	$y=3.27475\times10^7x-57539.21$	0.99	3.27475×10^7
1,4-Dimethylcyclohexane	$y=3.51508\times10^7x-32490.56$	1.00	3.51508×10^7
Benzene	$y=1.95320\times10^7x-12530.75$	0.98	1.95320×10^7
Toluene	$y=2.78540\times10^7x+4875.62$	0.99	2.78540×10^7
Xylene	$y=3.17429\times10^7x+17844.23$	1.00	3.17429×10^7
Cyclohexanedicarboxylic acid	$y=1.18650\times10^7x-8235.91$	0.97	1.18650×10^7
p-Toluic acid	$y=1.50230\times10^7x+2150.84$	0.98	1.50230×10^7
Cyclohexanecarboxylic acid	$y=1.79460\times10^7x-15320.35$	0.98	1.79460×10^7
4-Methyl cyclohexane methanol	$y=2.30210\times10^7x+9875.43$	0.99	2.30210×10^7
Cyclohexane methanol	$y=2.09875\times10^7x-5120.68$	1.00	2.09875×10^7
4-Hydroxymethyl-cyclohexane-1-carboxylic acid	$y=1.64280\times10^7x-9245.31$	0.98	1.64280×10^7
4-(ethoxycarbonyl)cyclohexane-1-carboxylic acid	$y=1.60345\times10^7x+8325.11$	0.97	1.60345×10^7
Ethyl 4-methylbenzoate	$y=2.18760\times10^7x+6543.27$	0.99	2.18760×10^7
Diethylterephthalate	$y=2.41230\times10^7x-19875.50$	0.99	2.41230×10^7

*y = peak area of species 'i'; x = mol of species 'i'.

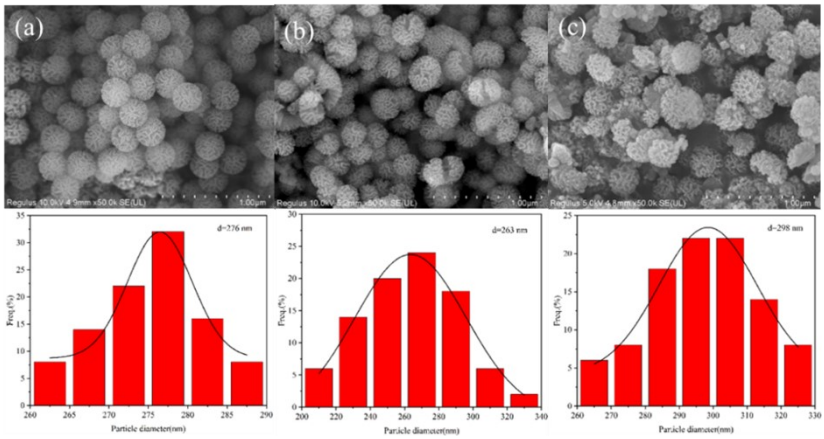

Fig. S1 SEM images and particle size distributions of (a) DFNS, (b) WO_3-DFNS (0.05), (c) WO_3-DFNS (0.1).

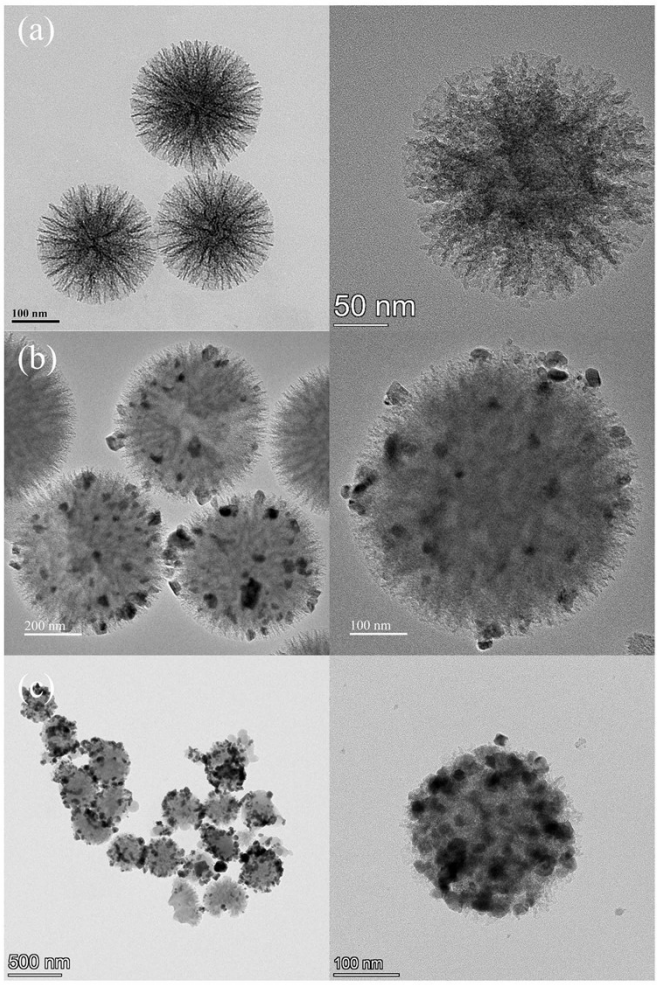

Fig. S2 TEM images of (a) DFNS, (b) WO_3-DFNS (0.05) and (c) WO_3-DFNS (0.1).

Table S2 The physical and chemical properties of the catalysts.

Catalyst	Composition(wt%) [a]		S_{BET} [b] ($m^2 \cdot g^{-1}$)	D_p [c] (nm)	V_p [d] ($cm^3 \cdot g^{-1}$)	d_{Ni} [e] (nm)
	Ni	W				
DFNS	-	-	520.9	10.1	1.9	-
WO_3-DFNS (0.05)	-	-	304.0	5.8	0.6	-
WO_3-DFNS (0.1)	-	-	184.7	6.4	0.4	-
Ni/DFNS	9.34	-	437.9	10.4	1.5	9.8
Ni/H_xWO_{3-y}-DFNS (0.05)	12.72	14.68	228.7	5.7	0.4	6.9
Ni/H_xWO_{3-y}-DFNS (0.1)	11.15	32.39	105.6	7.1	0.2	7.7

[a] Measured by ICP-AES;

[b] Surface areas of the catalysts based on the BET equation;

[c] Pore volumes of the catalysts derived from the volume of N_2 adsorbed at $p/p_0 = 0.99$;

[d] Average pore sizes calculated by the BJH method using the desorption branch;

[e] Ni nanoparticle size estimated from Ni (111) plane using the Debye-Scherrer equation.

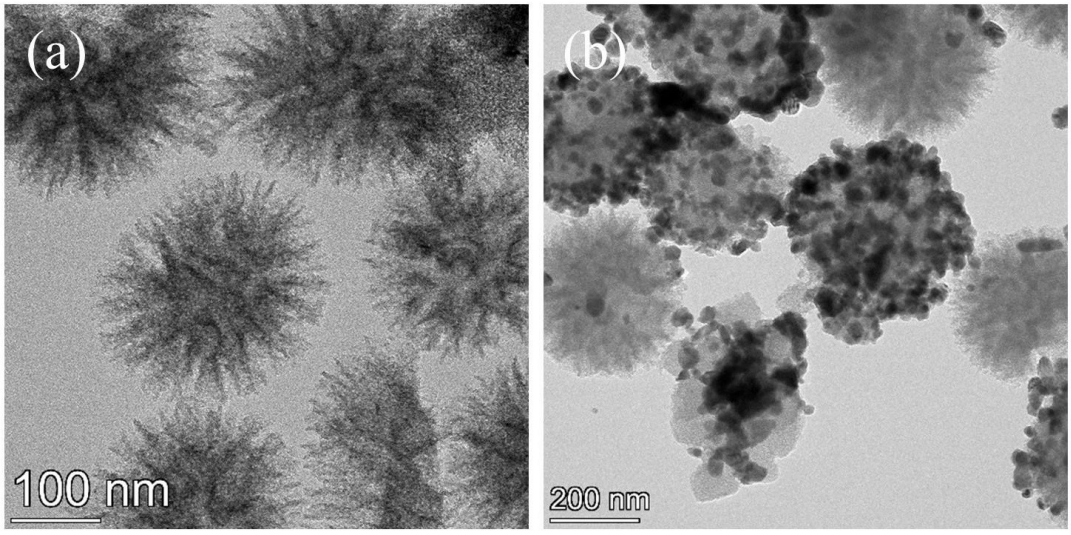

Fig. S3 TEM images of (a) Ni/DFNS and (b) Ni/H_xWO_{3-y}-DFNS (0.1).

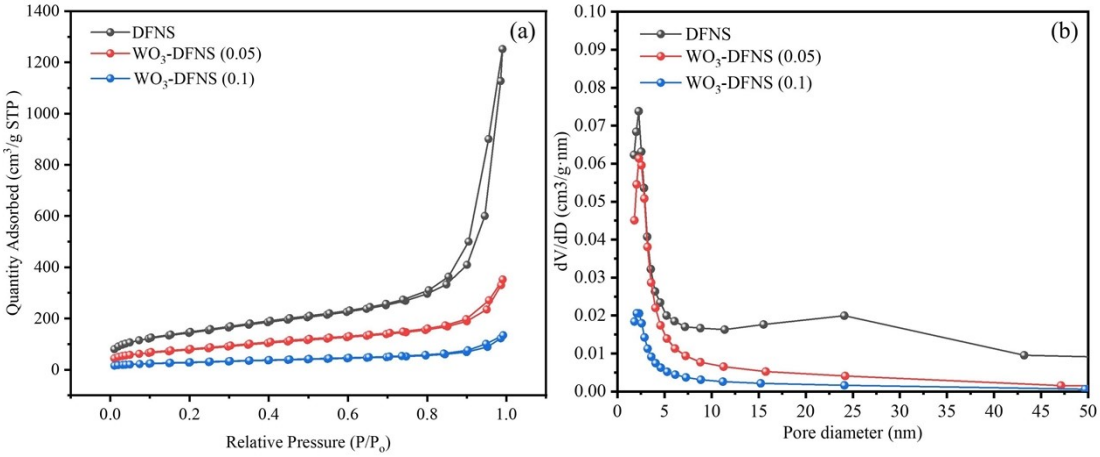

Fig. S4 (a) N_2 adsorption/desorption isotherms of catalysts and (b) pore size distribution of catalysts.

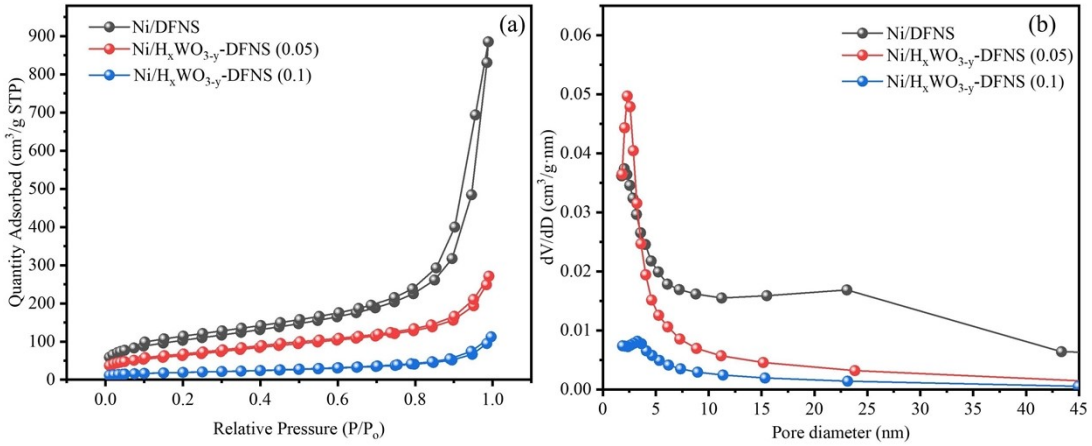

Fig. S5 (a) N_2 adsorption/desorption isotherms of catalysts, (b) pore size distribution of catalysts.

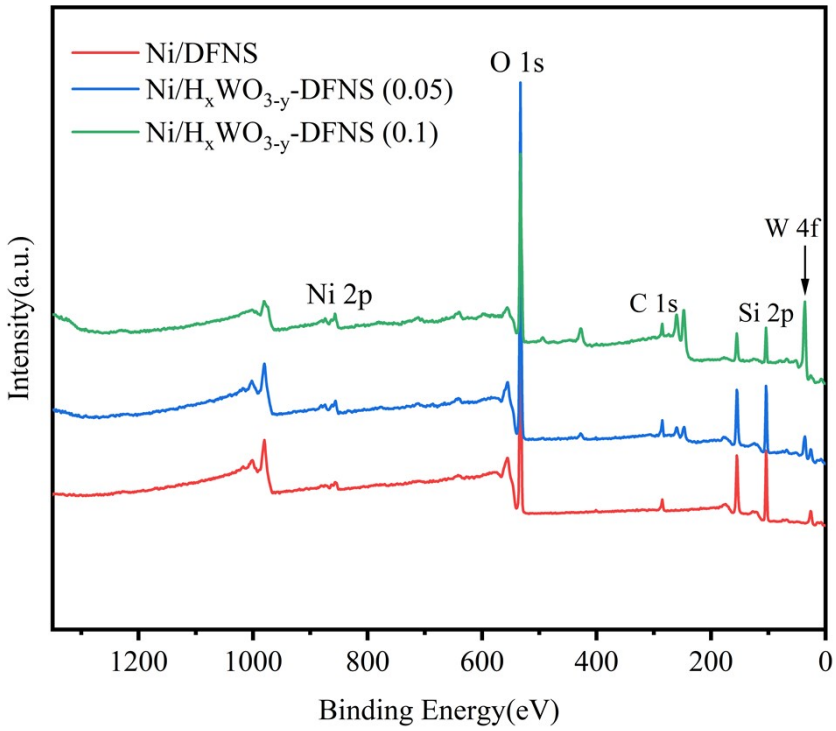

Fig. S6 XPS survey spectra of Ni/DFNS, Ni/H_xWO_{3-y}-DFNS (0.05) and Ni/H_xWO_{3-y}-DFNS (0.1).

Table S3 H_2-TPR results over Ni/DFNS, Ni/H_xWO_{3-y}-DFNS (0.05) and Ni/H_xWO_{3-y}-DFNS (0.1).

Entry	Catalyst	Ni amount/ mmol g_{cat}^{-1}	H_2-TPR	
			H_2 consumption/ mmol g_{cat}^{-1}	Valence of Ni
1	Ni/DFNS	1.60	1.56	0.05
2	Ni/H_xWO_{3-y}-DFNS (0.05)	2.16	1.99	0.10
3	Ni/H_xWO_{3-y}-DFNS (0.1)	1.90	1.82	0.08

Table S4 H_2-TPD results over Ni/DFNS, Ni/H_xWO_{3-y}-DFNS (0.05) and Ni/H_xWO_{3-y}-DFNS (0.1).

Sample	Peak Position (°C)		H_2 desorption amount (μmol/g_{cat})		
	Peak 1[a]	Peak 2[a]	Peak 1[a]	Peak 2[a]	Total
Ni/DFNS	145	592	7.3	0	7.3
Ni/H_xWO_{3-y}-DFNS (0.05)	138	624	14.7	15.0	29.7
Ni/H_xWO_{3-y}-DFNS (0.1)	137	606	19.5	6.7	26.2

[a] Peak 1 was the desorption peak of H species adsorbed on Ni sites.

[b] Peak 2 was the desorption peak of H species migrated to support.

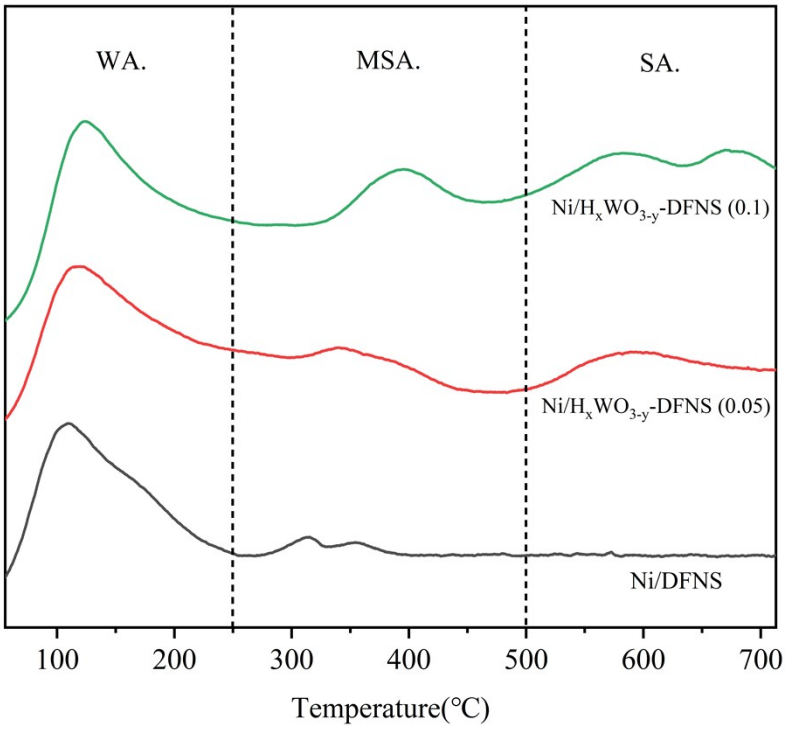

Fig. S7 NH_3-TPD spectra of Ni/DFNS, Ni/H_xWO_{3-y}-DFNS (0.05) and Ni/H_xWO_{3-y}-DFNS (0.1). WA.: Weak Acid, MSA.: Medium Strong Acid, SA.: Strong Acid.

Table S5 Quantified acid sites based on NH_3-TPD of Ni/DFNS, Ni/H_xWO_{3-y}-DFNS (0.05) and Ni/H_xWO_{3-y}-DFNS (0.1).

Catalysts	WA. (umol/g)	MSA. (umol/g)	SA. (umol/g)	Total acid sites (μmol/g)
Ni/DFNS	13	1	0	14
Ni/H_xWO_{3-y}-DFNS (0.05)	14	1	2	18
Ni/H_xWO_{3-y}-DFNS (0.1)	16	2	3	21

WA.: Weak Acid, MSA.: Medium Strong Acid, SA.: Strong Acid.

Table S6 Comparison of reported heterogeneous catalysts for HDO of PET with this work.

Catalysts	Temp (℃)	P (MPa)	T (h)	Products	Yield of aromatics or C_6-C_8 cycloalkanes (%)	Energy economy (ε) ($°C^{-1}*min^{-1}$)	Ref.
Co/TiO_2	320	3.0	24	Aromatics	75.2	1.36E-04	1
Ru/Nb_2O_5	320	0.5	16	Aromatics	83.6	2.72E-04	2
Ru/ZrO_2	200	0.3	12	Aromatics	36.8	2.56E-04	2
Ru/Nb_2O_5	220	2.0	12	Aromatics	92.4	5.83E-04	3
$Pt/NiAl_2O_3$	220	2.0	12	Aromatics	3.6	2.27E-05	3
$Pd/NiAl_2O_3$	220	2.0	12	Aromatics	21	1.33E-04	3
Ru/TiO_2	230	0.3	12	Aromatics	77.0	4.65E-04	4
Ru-Cu/SiO_2	400	6.0	22	Cycloalkanes	98.4	1.86E-04	5
Ru-280/Fe-N-C-800	350	5.0	4	Aromatics	82.6	9.83E-04	6
Ru/TiO_2	220	5.0	12	Cycloalkanes	87.9	5.55E-04	7
Ru/TiO_2	180	6.0	10	Cycloalkanes	72.9	6.75E-04	8
Ni/HZSM-5	240	4.0	4	Cycloalkanes	99.9	1.73E-03	9
Ru-ReO_x/SiO_2 + HZSM-5	190	3.0	20	Cycloalkanes	90.0	3.95E-04	10
Ir-ReO_x/SiO_2 + HZSM-5	190	3.0	4	Cycloalkanes	98.4	2.16E-03	11
Ni/H_xWO_{3-y}-DFNS (0.05)	280	5.0	16	Cycloalkanes	98.2	3.65E-04	This work

$\varepsilon = \frac{Y}{T \times t}$, where *Y* is yield of the main monomer, *T* is temperature of the reaction in degrees Celsius and *t* is reaction time (in minutes).

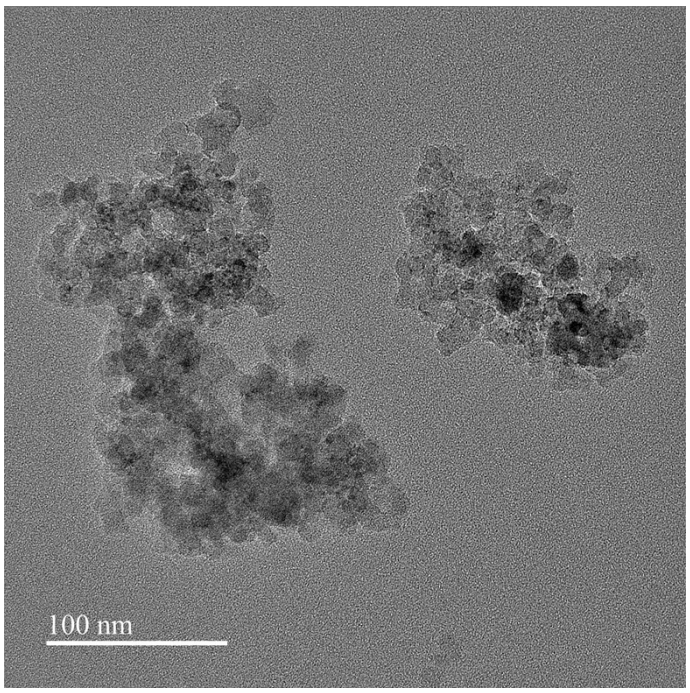

Fig. S8 TEM image of Ni-WO_x/SiO_2.

The initial depolymerization products were analyzed using an LC-Orbitrap-MS system (Q Extract Focus, Thermo Fisher Scientific) equipped with an Electrospray Ionization (ESI) detector. After the reaction, the solid and liquid phases in the reaction mixture were separated by centrifugation, and the solid phase was retained. Tetrahydrofuran (THF) was added to the solid phase to dissolve the initial PET depolymerization products, followed by another centrifugation step. The resulting liquid was filtered with 0.22 μm organic membrane filters and injected into a 100 × 2.1 mm ACQUITY UPLC BEH C_{18} column at a column temperature of 35 °C. The mobile phase consisted of a mixture of methanol (MeOH) and water. The flow rate was 0.3 mL min^{-1}. The products were eluted by the following gradients: 1 min isocratic at 10:90 (V/V) MeOH/H_2O, followed by a linear gradient to 100% (V/V) MeOH from 1 to 5 min, and finally held at 100% (V/V) MeOH from 5 to 30 min. The injection volume was 10 μL.

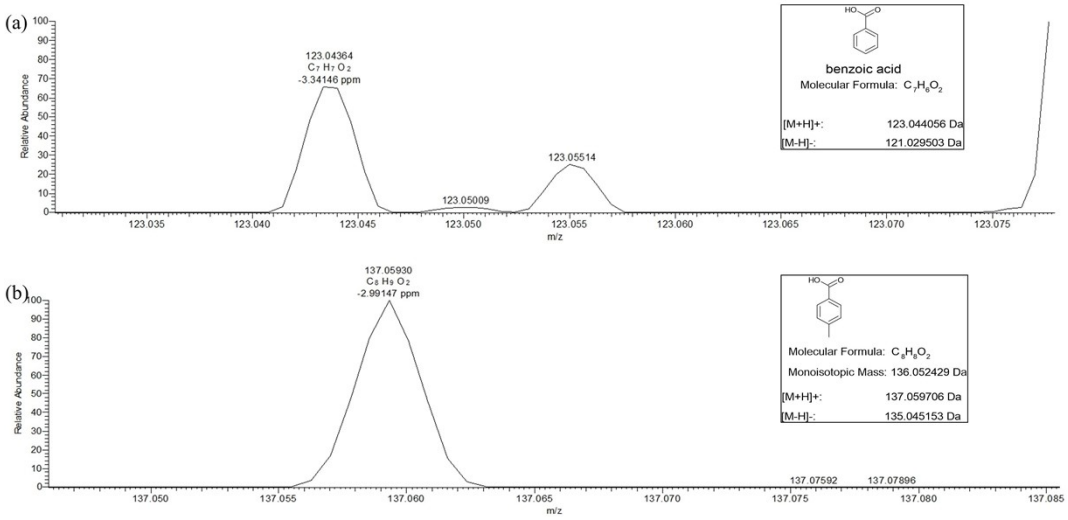

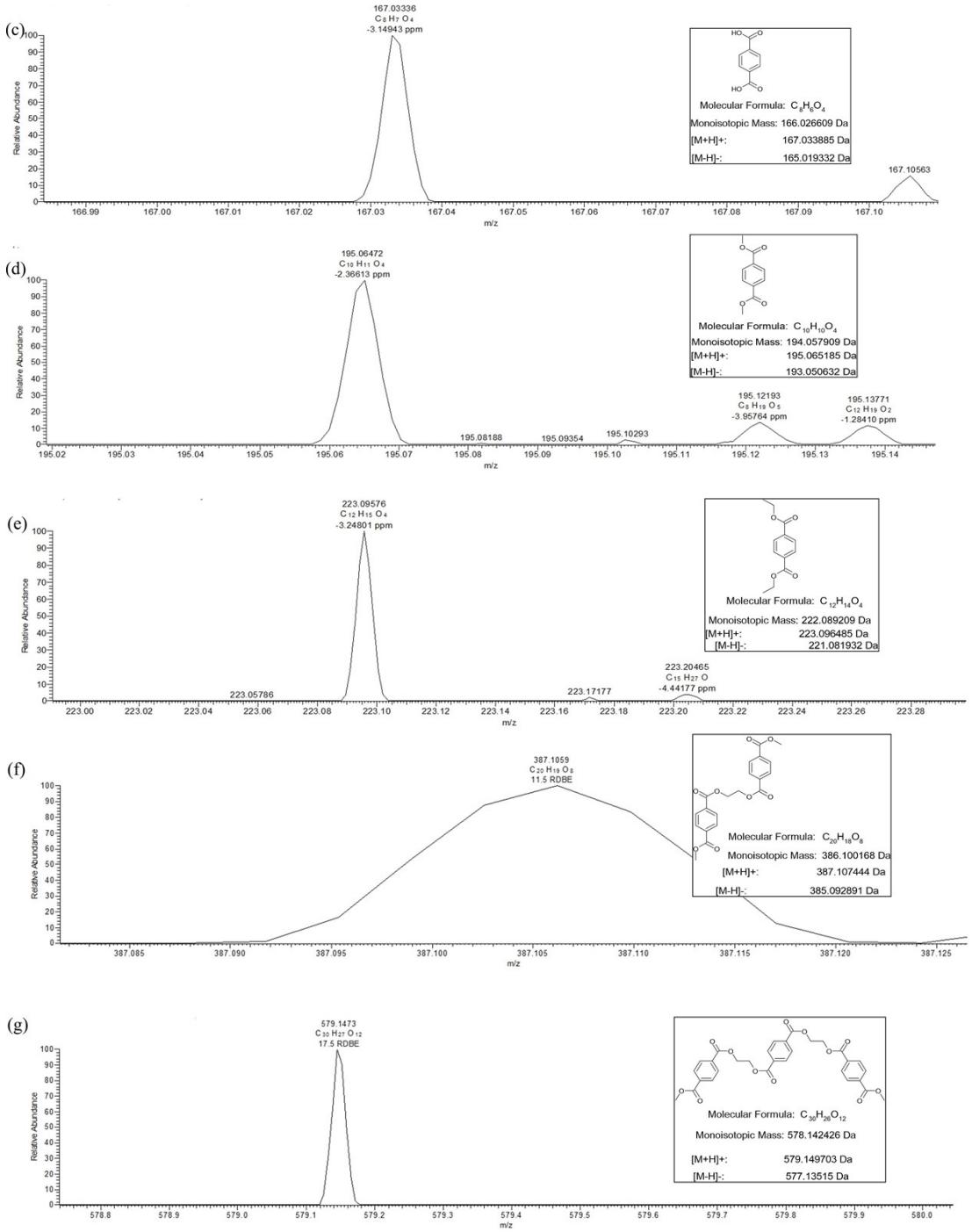

Fig. S9 The structures of the intermediates from HDO of PET over the Ni/H_xWO_{3-y}-DFNS (0.05) catalyst based on the LC-MS. Reaction condition: 0.05 g catalyst, 0.15 g reactant, 10 mL n-dodecane, 280 ℃, 5.0 MPa H_2.

Table S7 Gas compositions obtained from HDO of dodecane and PET in n-dodecane

Run	Gas concentration (mol%)			
	CO	CH_4	CO_2	C_2H_6
n-dodecane	0	2.9	0	0.70
PET in n-dodecane	0.3	3.8	2.5	1.5

Reaction condition: 280 ℃, 5.0 MPa H_2 for 16 h.

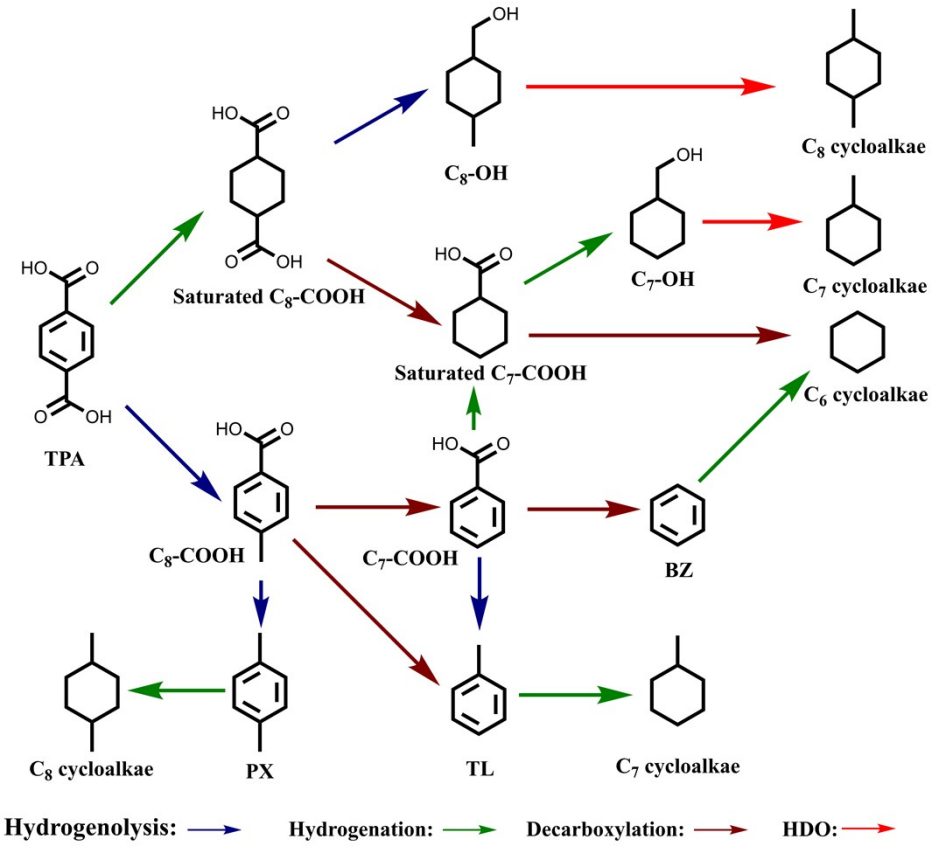

Fig. S10 Reaction pathway for HDO of TPA over the Ni/H_xWO_{3-y}-DFNS (0.05) catalyst. Reaction condition: 0.05 g catalyst, 0.15 g reactants, 10 mL n-dodecane, 260 ℃, 5.0 MPa H_2.

Table S8 Reaction rates of different model compounds over Ni/H_xWO_{3-y}-DFNS (0.05) catalyst[a].

Entry	Substrate	Rate / mmol g_{cat}^{-1} min^{-1}
1	TPA	4.65
2	C_8-COOH	2.43
3	C_8-OH	0.75

[a] Reaction conditions: 0.05 g catalyst, 0.15 g reactants, 10 mL n-dodecane, 260 ℃, 5.0 MPa H_2.

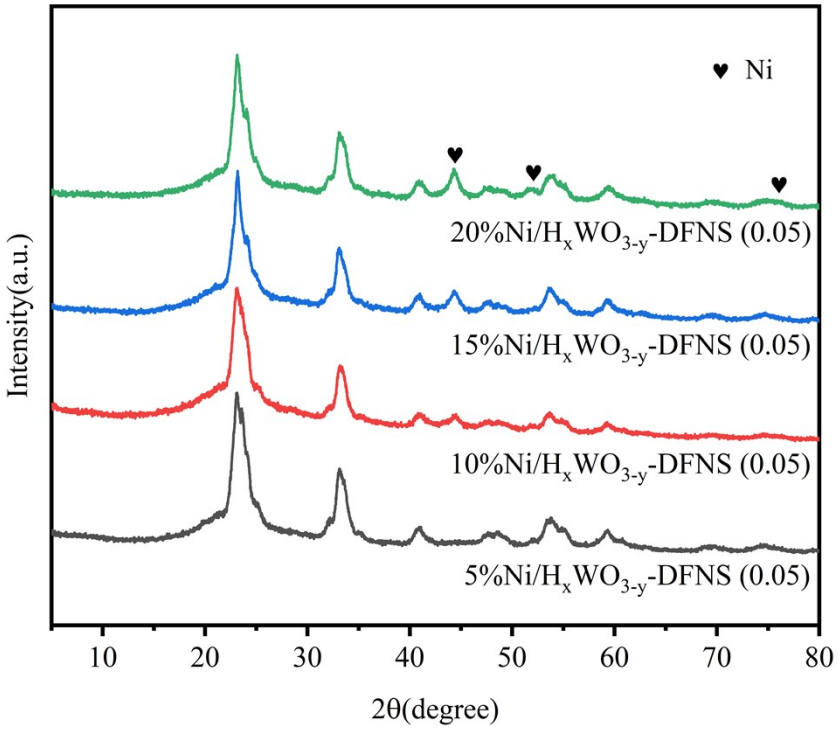

Fig. S11 XRD patterns of different catalysts.

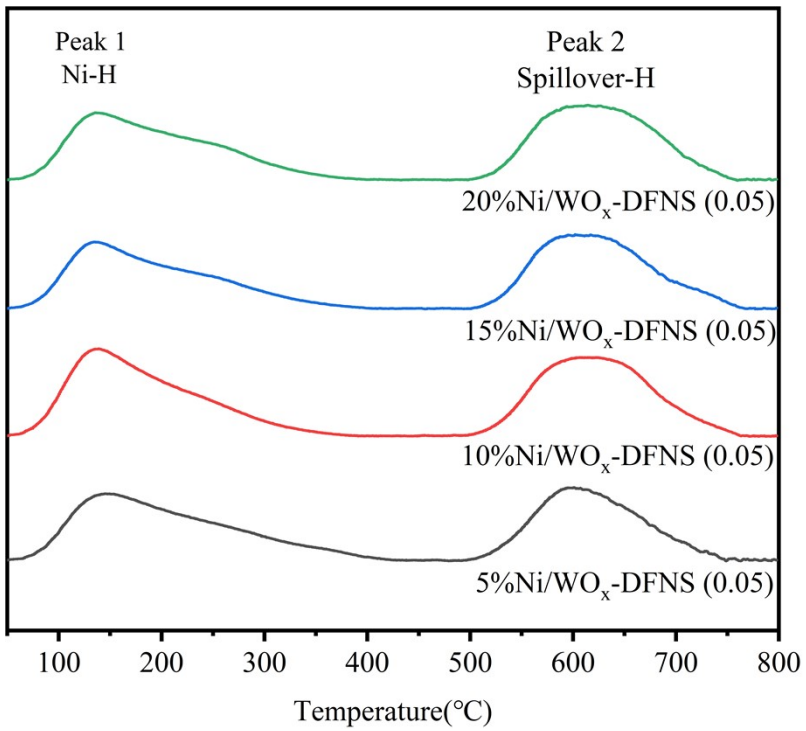

Fig. S12 H_2-TPD profiles of different catalysts.

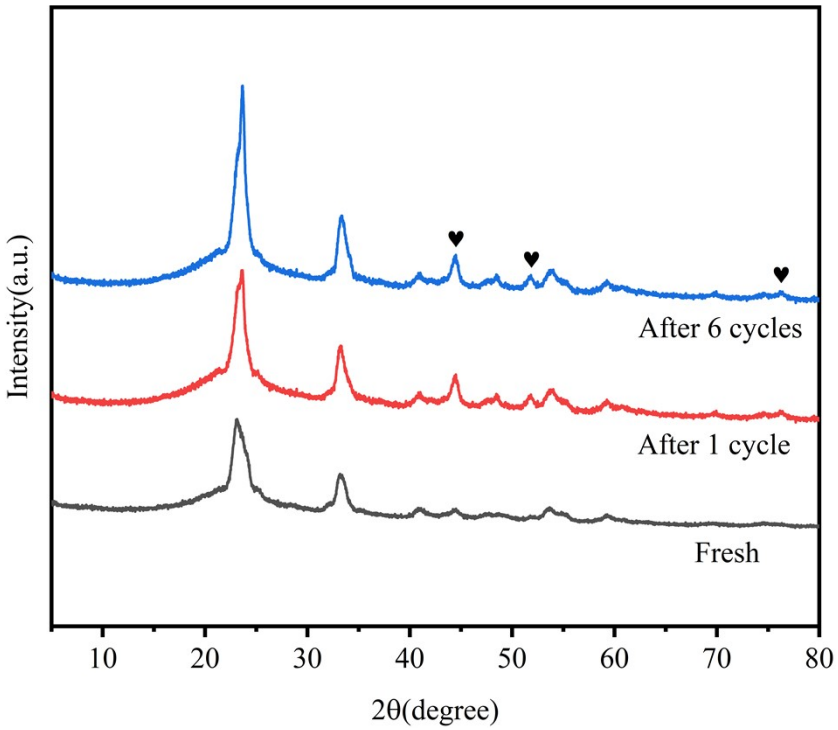

Fig. S13 XRD patterns of Ni/H_xWO_{3-y}-DFNS (0.05) and recovered catalyst after 2 and 4 cycles.

Supplementary references

1. S. Hongkailers, Y. Jing, Y. Wang, N. Hinchiranan and N. Yan, *ChemSusChem*, 2021, **14**, 4330-4339.
2. Y. Jing, Y. Wang, S. Furukawa, J. Xia, C. Sun, M. J. Hülsey, H. Wang, Y. Guo, X. Liu and N. Yan, *Angew. Chem. Int. Ed.*, 2021, **60**, 5527-5535.
3. S. Lu, Y. Jing, B. Feng, Y. Guo, X. Liu and Y. Wang, *ChemSusChem*, 2021, **14**, 4242-4250.
4. M. Ye, Y. Li, Z. Yang, C. Yao, W. Sun, X. Zhang, W. Chen, G. Qian, X. Duan and Y. Cao, *Angew. Chem.*, 2023, **135**, e202301024.
5. H. Tang, N. Li, G. Li, A. Wang, Y. Cong, G. Xu, X. Wang and T. Zhang, *Green Chem.*, 2019, **21**, 2709-2719.
6. J. Li, Z. An, Y. Kong, L. Zhang, J. Yang, X. Wang, J. Wang, D. Duan, Q. Zhang, R. Long, D. G. Vlachos and Z. Li, *Appl. Catal. B: Environ.*, 2024, **357**, 124307.
7. V. Murali, J. R. Kim, Y.-K. Park, J.-M. Ha and J. Jae, *Green Chem.*, 2023, **25**, 8570-8583.
8. R. Li, W. Zeng, R. Zhao, Y. Zhao, Y. Wang, F. Zhang, M. Tang, Y. Wang, X. Chang and F. Wu, *Nano Res.*, 2023, **16**, 12223-12229.
9. J. Liu, N. Wang, S. Liu and G. Liu, *JACS Au*, 2024, **4**, 4361-4373.
10. J. Wei, M. Zhu, B. Liu, N. Wang, J. Liu, K. Tomishige, S. Liu and G. Liu, *Angew. Chem. Int. Ed.*, 2023, **62**, e202310505.
11. N. Wang, J. Liu, J. Wei, S. Liu and G. Liu, *Sci. China Chem.*, 2024, 1-13.